



HAL
open science

Time-domain FWI of full azimuth OBN data from offshore North West Australia

Serge Sambolian, Romain Brossier, Ludovic Métivier

► **To cite this version:**

Serge Sambolian, Romain Brossier, Ludovic Métivier. Time-domain FWI of full azimuth OBN data from offshore North West Australia. 84th EAGE Annual Conference & Exhibition, Jun 2023, Vienne, Austria. pp.1-5, 10.3997/2214-4609.202310901 . hal-04278831

HAL Id: hal-04278831

<https://hal.science/hal-04278831>

Submitted on 10 Nov 2023

HAL is a multi-disciplinary open access archive for the deposit and dissemination of scientific research documents, whether they are published or not. The documents may come from teaching and research institutions in France or abroad, or from public or private research centers.

L'archive ouverte pluridisciplinaire **HAL**, est destinée au dépôt et à la diffusion de documents scientifiques de niveau recherche, publiés ou non, émanant des établissements d'enseignement et de recherche français ou étrangers, des laboratoires publics ou privés.

Time-domain FWI of full azimuth OBN data from offshore North West Australia

S. Sambolian^{1*}, R. Brossier¹, L. Métivier^{1,2}

¹ Univ. Grenoble Alpes, ISTERre, F-38058 Grenoble, France

² CNRS, Univ. Grenoble Alpes, LJK, F-38058 Grenoble, France

January 20, 2023

Main objectives

Perform full waveform inversion of a newly provisioned multi-component full-azimuth OBN broadband dataset. Evaluate the results and make an assesment serving as baseline for future multi-parameter inversions under the elastic approximation and multi-component polarization-based inversions.

New aspects covered

Pioneering work on a new dataset. Design and application of an FWI workflow to newly provisioned data from the Gorgon Field (North West Australia).

Summary (200 words)

Full waveform inversion of full-azimuth broadband ocean bottom nodes is emerging as the go-to strategy for high-resolution seismic imaging in marine settings. The areal extent of node acquisitions and the high signal-to-noise ratio at low frequencies fosters the illumination and undershooting of sought structures by deeply penetrating diving waves and post-critical reflections even in complex environments. In this work, we present full waveform inversion results of a newly provisioned full-azimuth broadband ocean bottom node data from the Gorgon field located off the northwest coast of Australia. We show that even at the first stage of the inversion, using conventional full waveform inversion, the P-wave vertical velocity model is significantly updated and reveals expected structural features in accordance with the geological setting of the Gorgon basin. The enhanced data fit and the excellent match of velocity profiles with well logs validates this result which will serve as baseline for ongoing and future multi-component and multi-parameter FWI of this dataset from offshore North West Australia.

Time-domain FWI of full azimuth OBN data from offshore North West Australia

Introduction

Full waveform inversion (FWI) is the leading seismic imaging method for building high-resolution subsurface parameter models (Virieux and Operto, 2009; Virieux et al., 2017). In marine settings, full-azimuth (FAZ) ultra-long offset seabed acquisitions have proven to be extremely beneficial in an FWI workflow due to the enhanced subsurface illumination compared to legacy datasets and the fostered undershooting of complex structures through deeply penetrating late arrivals (e.g. diving waves and post-critical reflections) (Shen et al., 2018). Furthermore, ocean bottom nodes (OBN) coupled with broadband sources give access to high-quality multi-component recordings with a high signal-to-noise ratio at frequencies ranging from as low as 1.5 Hz and up to 200 Hz (Blanch et al., 2020).

In this study, we present the first results obtained through full-waveform inversion of broadband full-azimuth ocean bottom node recordings from the Gorgon field, originally acquired in late 2015 to early 2016 and recently provisioned to us. At this stage, only pressure data are inverted to update solely the P-wave vertical velocity under the acoustic approximation, with the assumption that the medium exhibits transverse isotropy with a vertical symmetry axis (VTI). We show, in the following, the updated P-wave vertical velocity model with an assessment through data and well log matching.

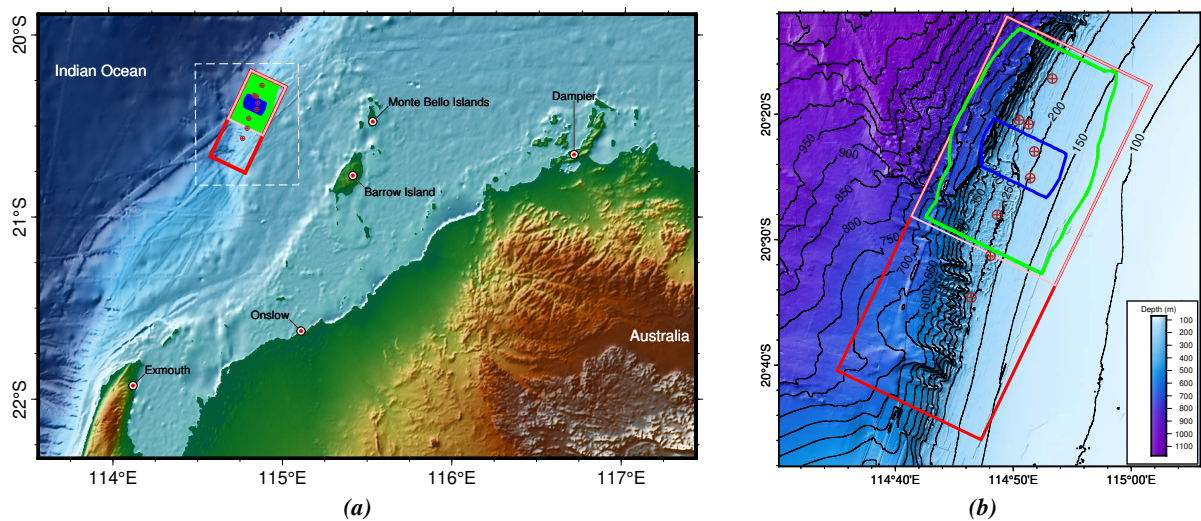


Figure 1 (a) Relief map of North West Australia. The blue and green dots represent the ocean bottom nodes and the shot carpet positions. The dashed white line delineates the area detailed further in panel b. (b) Bathymetry map of the North West Shelf of Australia. The bathymetry was compiled by Lebec et al. (2021) and obtained via AusSeabed (www.ausseabed.gov.au). The acquisition coverage area is outlined by the green and blue polygons. In both panels, the red and pink rectangles delineate the original imaging area and this study's model extent. The brown target marks highlight wells positions.

The Gorgon case study

Geological context, acquisition design and subsurface models

The Gorgon field is located in the Northern Carnarvon basin, approximately 130 km of the north-western coastline of Australia. The original rolling on/off acquisition is comprised of 697350 shotpoints and 3099 4C-OBNs covering a 238 km² full fold area (Figure 1, red rectangle). The shots and nodes were positioned following a 37.5 m and 375 m staggered grid, respectively. The recordings provided to us are limited to 650 OBN and their corresponding shotpoints (Figure 1a, blue and green dots). The sources were towed at 9 m below sea level while the OBN positions follow the highly varying seabed topography (Figure 1b). The high resolution bathymetry collection, originally compiled by Lebec et al. (2021), was obtained via AusSeabed (www.ausseabed.gov.au). The field, discovered a couple of decades ago, was appraised through numerous wells of which seven were provided to us (Figure 1, brown target marks). The geological setting of the area is characterized by a complex NE-SW trending fault

system, with the main structure being the 45 km long Triassic elevated block referred to as the Gorgon horst. The latter structure is bounded by major faults which offer closure for the gas-rich Mungaroo Formation sands present at depths ranging from 3.3 to 4.6 km and the top of the block is defined by the Intra-Jurassic Unconformity (IJU) (Chongzhi et al., 2013). In fact, the provided subsurface parameters models already contain strong imprints of the Gorgon horst bounds as illustrated in Figure 2.

The initial P-wave vertical velocity model V_{P0} contains a wedge-like low velocity layer ($\approx 2.2 \text{ km.s}^{-1}$) present at 2 km depth bounded by a tabular layer with wavespeeds up to 3.2 km.s^{-1} from the top and a high velocity gradually increasing from its bottom down to the IJU at the top of the horst. The alternating positive-negative velocity gradient acts as a suspected wavefield trap between the high velocity layer and the horst; the latter effect along with the rough and strongly varying seabed makes the data anatomy challenging to decrypt without full waveform modelling and a good understanding of the local stratigraphical setting. The VTI parameters depict moderate anisotropy from 2 km depth down to the top of the horst in δ while it extends down to 6 km with mild values of ϵ . Using the initial V_{P0} model, we build a density model through Brocher's polynomial law (Brocher, 2005).

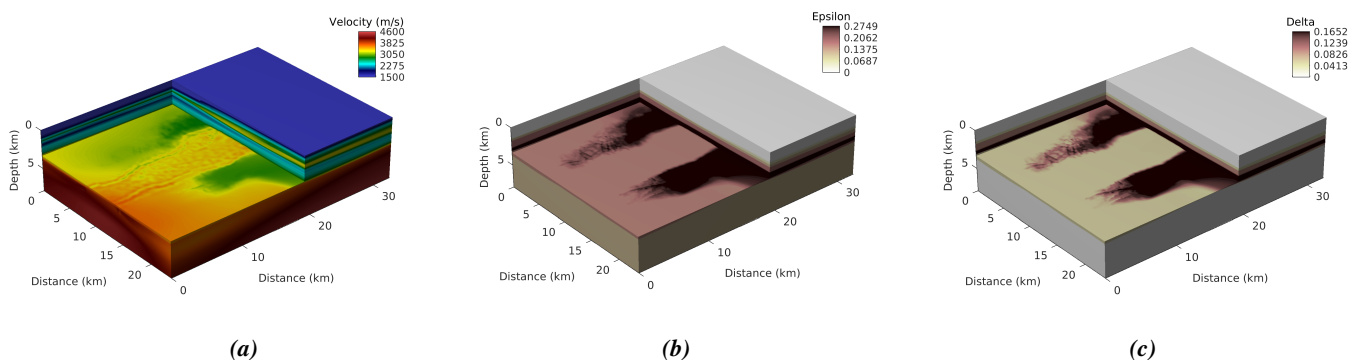


Figure 2 Initial (a) P-wave vertical velocity model V_{P0} and the anisotropy parameters (b) ϵ and (c) δ . Subset of the model removed to show the low velocity layer at 2 km depth the imprint of the Gorgon horst bounds at the Intra-Jurassic Unconformity (IJU) level (3.2 km depth).

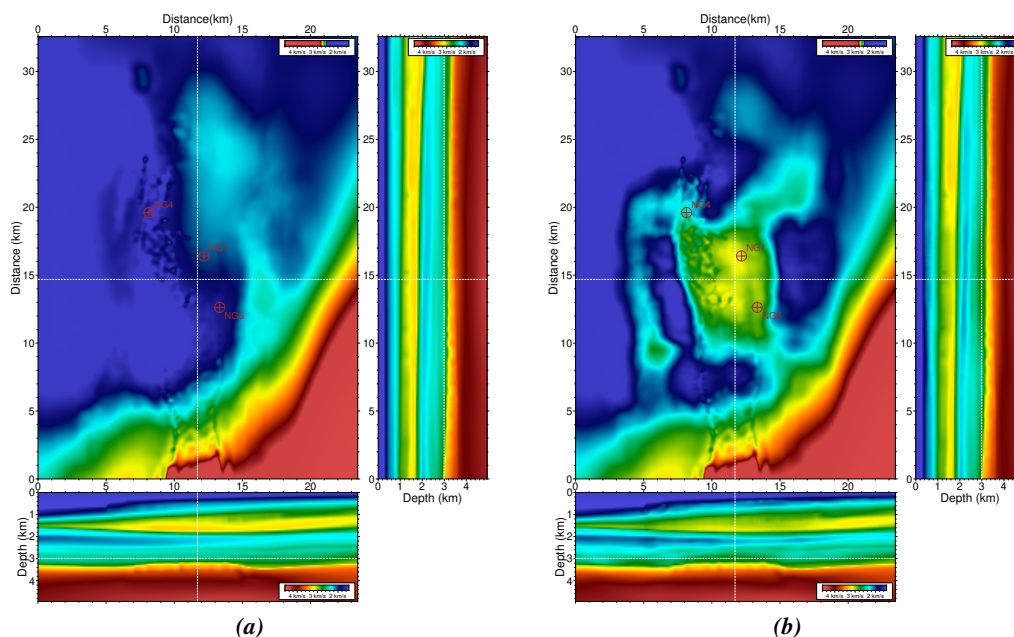


Figure 3 Slices from the (a) initial and (b) updated V_{P0} models. The white dashed lines delineates the extraction profiles. Vertical depth-varying slices are taken through the middle of the OBN coverage and the horizontal constant-depth slice is taken at 3 km depth. The brown target marks highlight the North Gorgon wells positions.

FWI setup and inversion results

The data provided to us were lightly pre-processed (e.g. debias and instrument inverse filters, positioning and orientation correction of the geophone components). We project the data coordinates to a local

coordinate system, apply source-receiver reciprocity and remove spiky traces. For the inversion in the first frequency band presented here, we apply a minimum-phase filter (1.75 - 5 Hz) to the hydrophone component followed with F-K filtering to remove coherent noise from some common-receiver gathers. Data are modelled in the models of Figure 2 followed by source wavelet estimation through linear deconvolution for each OBN. During source estimation, the common-receiver gathers are muted following an automatically designed time-offset window around the short-offset direct arrival.

We proceed with a full batch FWI of the whole data. It should be noted that we use a time-domain modelling finite-difference based engine and that a frequency-domain FWI on the same case study was recently performed (Operto et al., 2022). We invert solely for V_{P0} while keeping other parameters unchanged. We use a preconditioned l -LBFGS algorithm for the optimization. In order to compensate for geometrical spreading and energy decay, a simple depth preconditioner is applied on the gradient. The latter step consists of scaling the gradient as a function of depth raised to the power of 1.25. The gradient is smoothed using a nonstationary wavelength adaptive Gaussian filter.

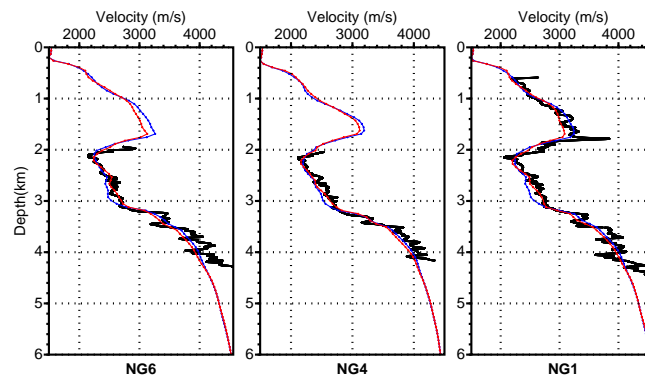


Figure 4 Velocity log profiles from wells: North Gorgon 6, North Gorgon 4 and North Gorgon 1 represented by the black dots. The blue and red lines represent the vertical profiles taken from the initial and updates models at the positions of the wells. Refer to Figure 3 for wells location.

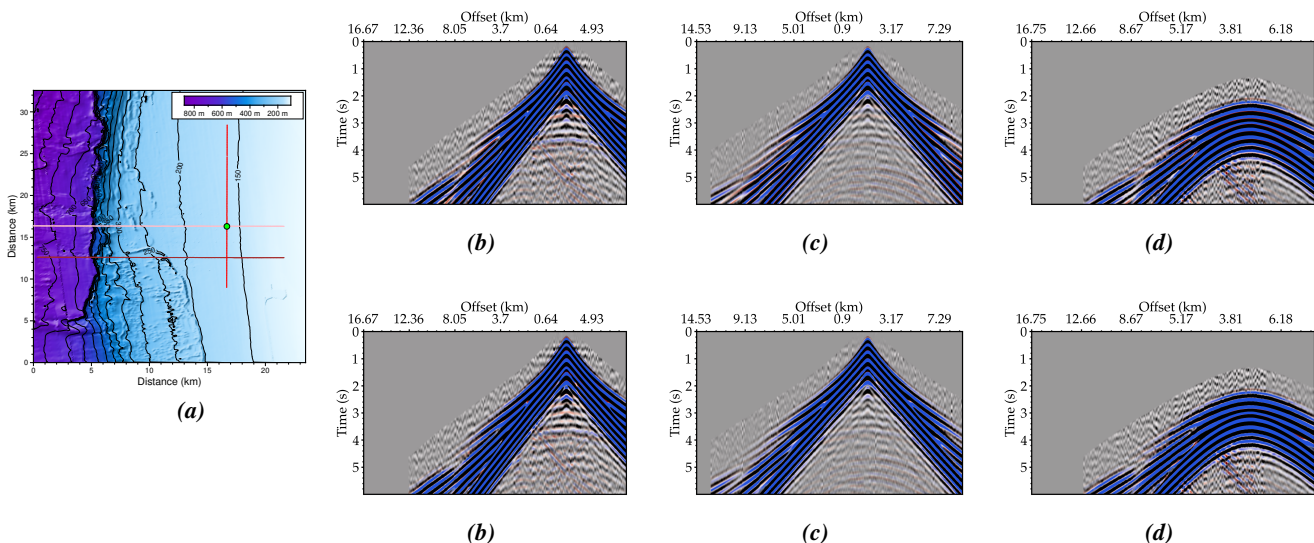


Figure 5 (a) Bathymetry map overlain by the position of all shots 2792 (red) and all shots from lines 4042 (pink) and 4442 (red), the green dot marks the position of OBN 196. (b-d) Comparison between recorded OBN 196 data (black and white) and simulated OBN 196 data (red and blue) in the initial model (top) and the FWI-derived model (bottom) for the pink, red and brown lines of (a), respectively.

Slices of the model obtained after 25 FWI iterations through the aforementioned workflow are presented in Figure 3. The vertical depth-varying slices are extracted at positions that intersects with the center of the OBN coverage area while the horizontal constant-depth slice is taken at 3 km which corresponds to the formation group on top of the IJU which already had an imprint in the initial model (Figure 2). This particular depth horizon is interesting due to the mismatch between the velocity profiles from the

initial model and the well logs (Figure 4, blue line at 3 km depth). In fact, the main objective at this frequency band is to correctly update the pre-IJU units before resolving the layers of the reservoir in the subsequent FWI at higher frequency bands. The constant-depth horizontal slice taken in the initial model (Figure 3a) show that there is a very slight imprint of the Gorgon horst in the vicinity of the wells. On the other hand, in the FWI model (Figure 3b) higher wavespeeds are seen in the same slice. The updates are actually consistent with the width of Gorgon horst below and the velocity trend is validated through well logs (Figure 4, red line). The varying-depth vertical slices from the FWI model reveal sharper interfaces between the contrasting high-low velocity layers compared with the initial model. The comparison between the recorded and simulated data in both models (Figure 5) illustrates the better data fit in terms of phase and amplitude at long offset. The post-critical reflection from the top of the horst, which was mostly updated in FWI, is recorded at 11 km offset, it is clearly the most enhanced part of the seismograms. At short offset, the simulated data do not fit the recordings in terms of amplitudes due to suspected misrepresented sea-bottom geometry and impedance contrast in very fine shallow layers. The latter is expected to be enhanced during inversions at higher frequency bands.

Ongoing work and conclusion

We present a first result from a novel case study from offshore North West Australia. We perform a time-domain mono-parameter FWI of the full-azimuth OBN hydrophone component data. The updates around the main horst block and the intermediate low-velocity layer in the FWI-derived model are validated through the well logs and the improved data fit. Ongoing higher frequency bands inversions resolve further the deep reservoir. In future inversions, a structurally-preserving anisotropic diffusion filter (Métivier and Brossier, 2022) will be used in order to preserve the sharp contrasts around the Gorgon horst (IJU and bounding faults). The presented result will serve as a baseline for multi-component polarisation-based FWI (Sambolian et al., 2022) and multi-parameter elastic FWI (Cao et al., 2022).

Acknowledgements

We thank CHEVRON and DUG for providing the Gorgon OBN dataset and all its peripheral products. This study was partially funded by the SEISCOPE consortium (<http://seiscope2.osug.fr>), sponsored by AKERBP, CGG, EXXON-MOBIL, GEOLINKS, JGI, PETROBRAS, SHELL, SINOPEC and TOTALENERGIES. This study was granted access to the HPC resources provided by the GRICAD infrastructure (<https://gricad.univ-grenoble-alpes.fr>), Cray Marketing Partner Network (<https://partners.cray.com>) and IDRIS/TGCC under the allocation 046091 made by GENCI.

References

- Blanch, J., Jarvis, J., Hurren, C., Kostin, A., Liu, Y. and Hu, L. [2020] Designing an exploration-scale OBN: Acquisition design for subsalt imaging and velocity determination. *The Leading Edge*, **39**(4), 248–253.
- Brocher, T.M. [2005] Empirical relationships between elastic wavespeeds and density in the earth's crust. *Bulletin of the Seismological Society of America*, **95**(6), 2081–2092.
- Cao, J., Brossier, R. and Métivier, L. [2022] Elastic full-waveform inversion of 4C ocean-bottom seismic data: Model parameterization analysis. In: *Second International Meeting for Applied Geoscience & Energy*. 957–961.
- Chongzhi, T., Guoping, B., Junlan, L., Chao, D., Xiaoxin, L., Houwu, L., Dapeng, W., Yuan, W. and Min, L. [2013] Mesozoic lithofacies palaeogeography and petroleum prospectivity in North Carnarvon Basin, Australia. *Journal of Palaeogeography*, **2**(1), 81–92.
- Lebrec, U., Paumard, V., O'Leary, M.J. and Lang, S.C. [2021] Towards a regional high-resolution bathymetry of the North West Shelf of Australia based on Sentinel-2 satellite images, 3D seismic surveys, and historical datasets. *Earth System Science Data*, **13**(11), 5191–5212.
- Métivier, L. and Brossier, R. [2022] On the use of nonlinear anisotropic diffusion filters for seismic imaging using the full waveform. *Inverse Problems*, **38**(11), 115001.
- Operto, S., Amestoy, P., Aghamiry, H.S., Beller, S., Buttari, A., Combe, L., Dolean, V., Gerest, M., Guo, G., Jolivet, P., L'Excellent, J.Y., Mamfoumbi, F., Mary, T., Puglisi, C., Ribodetti, A. and Tournier, P.H. [2022] Does 3D frequency-domain FWI of full-azimuth/long-offset OBN data feasible? The Gorgon case study. *arXiv*.
- Sambolian, S., Brossier, R. and Métivier, L. [2022] Exploiting the richness of multi-component data: a time-dependent polarization-based FWI approach. In: *83rd Annual EAGE Meeting (Madrid)*. European Association of Geoscientists & Engineers.
- Shen, X., Ahmed, I., Brenders, A., Dellinger, J., Etgen, J. and Michell, S. [2018] Full-waveform inversion: The next leap forward in subsalt imaging. *The Leading Edge*, **37**(1), 67b1–67b6.
- Virieux, J., Asnaashari, A., Brossier, R., Métivier, L., Ribodetti, A. and Zhou, W. [2017] An introduction to Full Waveform Inversion. In: Grechka, V. and Wapenaar, K. (Eds.) *Encyclopedia of Exploration Geophysics*, Society of Exploration Geophysics, R1–1–R1–40.
- Virieux, J. and Operto, S. [2009] An overview of full waveform inversion in exploration geophysics. *Geophysics*, **74**(6), WCC1–WCC26.